

A METHOD TO DESIGN DUAL-BAND, HIGH-DIRECTIVITY EBG RESONATOR ANTENNAS USING SINGLE-RESONANT, SINGLE-LAYER PARTIALLY REFLECTIVE SURFACES

Y. Ge and K. P. Esselle

Centre for Microwave and Wireless Applications
Electronic Engineering
Macquarie University
Sydney, NSW 2109, Australia

T. S. Bird

CSIRO ICT Centre
P. O. Box 76, Epping, NSW 1710, Australia

Abstract—A new method is presented to design *dual-band*, high-directivity, EBG-resonator antennas using simple, *single-resonant*, single-layer partially reflective surfaces (PRS). The large, positive gradient of the reflection phase versus frequency curve of partially reflecting surfaces, observed only close to the resonance frequency of the PRS, is exploited for this purpose. An example single-resonant PRS, based on a frequency-selective surface (FSS) composed of a printed slot array, was designed. Then it is used to design an EBG-resonator antenna to demonstrate the feasibility of achieving *dual-band* performance. Cavity models are employed, together with the reflection characteristics of the PRS, to understand the operation of the device at critical frequencies such as cavity resonance frequencies and the PRS resonance frequency. Antenna simulations and computed results confirm the dual-band operation of this very simple, single-layer, low-profile EBG-resonator antenna. It resonates in two bands centered at 10.5 GHz and 12.3 GHz. The peak directivity in each band is 18.2 dBi and 20.5 dBi, and the 3 dB directivity bandwidth of each band is 7.5% and 8.7%, respectively.

Corresponding author: Y. Ge (yuehe@ics.mq.edu.au).

1. INTRODUCTION

In recent years, microwave applications based on electromagnetic band gap (EBG) structures have attracted significant attention [1, 2]. An important application of EBGs is the realization of high-gain low-profile antennas with a Fabry-Perót resonator [1–10], providing a low-profile aperture antenna. 1-D, 2-D and 3-D EBG structures have been investigated for this purpose [3–5]. Most of the 2-D EBG resonator antennas are based on frequency selective surfaces (FSS), which also behave as partially reflective surfaces (PRS) at the antenna operating frequencies [6–10]. The advantages of FSS, especially when employed to realize *single-band* EBG resonator antennas, are simplicity, low cost, ease of fabrication and ease of mounting. It is easy to change their properties, such as the reflection magnitude and phase, and by optimizing them, EBG resonator antennas with good performance can be realized.

EBG and FSS structures have in the past been applied to design *dual-band* EBG resonator antennas [6–10]. For instance, an EBG superstrate made out of triple-layer dielectric cylindrical rods was employed in one dual-band design [6]. Two operating bands can be obtained by the insertion of defect rods in the EBG. In another example, a FSS structure made out of a single dielectric layer with two strip-dipole arrays on its two surfaces was proposed as a superstrate for dual-band EBG resonator antennas [7]. In [8, 9], the FSS structure was considered as a ground to generate a reflection phase jump at the design frequency. Two frequency bands are obtained when a cavity is formed using such a FSS ground and a single layer superstrate. Dual-band EBG antennas can also be designed using a double-layer EBG superstrate [10]. When the cavity height and the distance between the two layers are appropriately selected, dual-band operation is expected.

In this paper, we propose a method to design a *single-layer* FSS that can be used to make a *dual-band* EBG resonator antenna when employed as a superstrate. For simplicity a standard PEC ground plane is assumed, although the design method is applicable to other types of ground planes such as PMCs. With this method, the designer can obtain the reflection phase characteristics required for a *dual-band* high-directivity EBG antenna, using a very simple, *single-band*, single-layer FSS such as a printed slot array. Hence the resulting *dual-band* EBG resonator antenna has advantages of simplicity, low cost, low profile, ease of fabrication and ease of mounting, just like their conventional *single-band* counterparts. An example design is presented to demonstrate the effectiveness of the proposed design method for dual-band EBG antennas. Section 2 outlines the basics

of EBG resonator antennas and the analysis methods employed here. The new design method for dual-band EBG antennas is detailed and demonstrated in Section 3. The radiation characteristics, such as directivity, of an example dual-band antenna design are presented in Section 4.

2. CHARACTERISATION OF EBG RESONATOR ANTENNAS

2.1. Characteristics of EBG Resonator Antennas

A typical 2D EBG resonator antenna, based on a FSS, is shown in Fig. 1. It consists of a superstrate, a ground plane and a feed antenna for excitation. The superstrate forms a FSS-based 2-D EBG structure where periodic conducting patterns are printed on one or both of its surfaces. It behaves as a partially reflective surface (PRS) at the antenna operating frequencies, and forms a resonant cavity together with the ground plane.

The gain of such an EBG resonator antenna is mainly determined by the area of the PRS, the reflection coefficient (magnitude and phase) of the PRS and the cavity height h , shown in Fig. 1. If the cavity resonance condition is satisfied, the maximum gain of the antenna will be achieved. The cavity resonance condition is associated with the reflection phases from the PRS and the ground, the propagation phase through the cavity (h), and the operating frequency. It is given by [2]

$$\phi_P + \phi_G - \frac{2\pi}{\lambda} 2h = 2k\pi, \quad k = 0, \pm 1, \pm 2 \dots \quad (1)$$

where ϕ_P and ϕ_G are reflection phases of PRS and the ground, respectively. This resonance condition ensures that all the waves arriving at the bottom surface of the PRS after multiple reflections are in-phase with the first incident wave. For a PEC ground, the reflection phase ϕ_G is always 180° for all frequencies of interest. If the height h

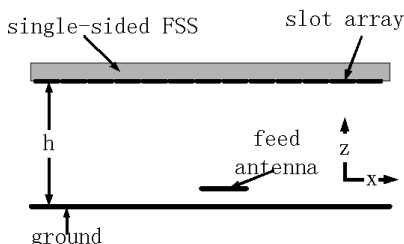


Figure 1. The configuration of a typical 2-D EBG resonator antenna.

is fixed, the cavity resonance frequencies are mainly determined by the reflection phase profile (i.e., phase versus frequency curve) of the PRS.

2.2. Method of Analysis

To analyze or design this type of antennas, we first apply the image theory to remove the ground plane. A cavity composed of the superstrate and its image will resonate at the same frequency as the antenna. Since the size of the feed antenna is considered much smaller than that of the superstrate and the ground, the effect of the small feed antenna on the resonant cavity can be ignored. Hence, the analysis of the PRS with a periodic configuration and the EBG resonator antenna can be reduced to a unit cell and a cavity model composed of only one cell, by applying periodic boundary conditions (PBC) [5]. A unit cell model is shown in Fig. 2(a), where the unit cell of a PRS is surrounded by four periodic boundaries. This model can be used to estimate the transmission and reflection of the PRS, under the normal incidence. Fig. 2(b) shows the resulting cavity model. It has a single cell of the periodic superstrate and its image surrounded by four periodic boundaries. The reduction of the analysis to a unit cell and its image significantly saves computational memory and time,

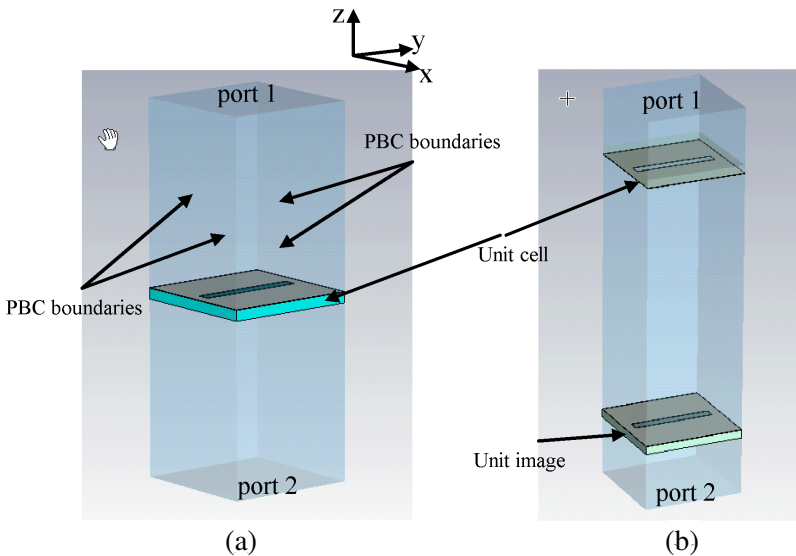


Figure 2. (a) A unit cell model for the PRS; (b) a cavity model composed of a unit cell and its image.

compared to the direct analysis of the whole EBG resonator antenna. For normal incidence, the periodic boundaries surrounding the unit cell or the unit cavity can be replaced by the PEC (perfect electric conductor) and PMC (perfect magnetic conductor) walls. For example, in the cases shown in Fig. 2(a), a slot is etched on one surface of the unit cell. The boundaries perpendicular to axis x should be set as PEC walls and those perpendicular to axis y should be PMC walls. Waveguide ports are placed on the two sides of the model. After these settings, x -polarised normal incidence will be applied to the CST or HFSS analysis.

In this research, the commercial software CST Microwave Studio has been used for the analysis and design of dual-band EBG resonator antennas.

3. A SINGLE-LAYER PRS FOR DUAL-BAND EBG RESONATOR ANTENNAS

3.1. Design Method

It is known that, when resonant inclusions are introduced to an object, it exhibits significantly different electromagnetic properties around the inclusion resonance frequency. Our previous investigations have confirmed that the reflection phase of a PRS can vary significantly around the inclusion resonance frequency when periodic resonant inclusions are embedded [11]. For example, the reflection phase of a typical PRS *slowly decreases* with frequency. However, if it contains a 2D array of resonant slots, the reflection phase *rapidly increases* with frequency around the first resonance frequency of the slots. Due to this highly distorted and inverted phase profile, it is possible to strategically design a PRS with a *single* inclusion resonance frequency in such a way that when it is employed in an EBG resonator antenna, the cavity resonance condition is satisfied at *two* frequencies. This means a dual-band antenna can be obtained from a *single-band* PRS! This design method and the theory behind it are further explained in subsequent sections, with example designs.

3.2. Design Example

A single-dielectric layer with a 2-D *slot* array is a *simple* example of PRSs that can be employed for this design method. For illustration, let us consider the single-layer PRS shown in Fig. 3. It is based on a single dielectric layer with a conductor coating on its bottom surface, which includes a 2-D periodic array of slots etched in the conductor coating.

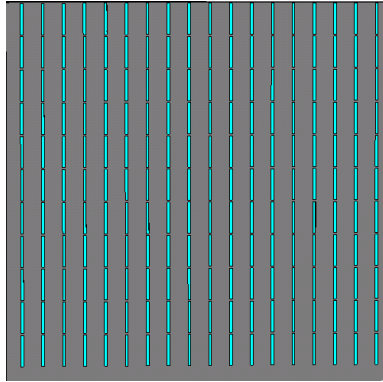


Figure 3. Configuration of the proposed PRS.

Let us also assume that the dielectric layer is made out of FR4/Epoxy material, which has a dielectric constant of about 4.4 and a thickness of 0.8 mm. The unit cell has initial dimensions of 10 mm \times 6 mm \times 0.8 mm. The etched slots on the bottom side have dimensions of 8 mm \times 0.2 mm. The reflection coefficient magnitude and phase of this PRS, obtained using the model shown in Fig. 2(a) and CST Microwave Studio, are plotted in Fig. 4. At 11.64 GHz, the reflection magnitude is very small because the slots (and hence the PRS) resonate at this frequency. The reflection phase *decreases slowly* with frequency for most frequencies but it *increases sharply* close to the slot resonance frequency. For comparison, the reflection phase of a normal PRS, (which could be used in a conventional *single-band* EBG resonator antenna,) is also plotted in Fig. 4. It has a *small, negative* slope and decreases gradually with increasing frequency.

Starting from resonance condition in Equation (1), one can derive an expression for the cavity height $h(f)$ that is required to make the cavity to resonate at a given frequency f . This is given by

$$h(f) = \frac{c}{4\pi f}(\phi_P + \phi_G - 2k\pi), \quad k = 0, \pm 1, \pm 2 \dots \quad (2)$$

where f denotes the frequency and c is light speed.

When the reflection phases of the PRS (ϕ_P) and the ground (ϕ_G , usually 180°) are known, it is possible to calculate the cavity height required to make the cavity to resonate at each frequency, using Equation (2). When this is done for the example PRS mentioned above, for all frequencies of interest, one obtains the relationship between the cavity height and cavity resonance frequency plotted in Fig. 5. To obtain the curves in Fig. 5, two different values of k need

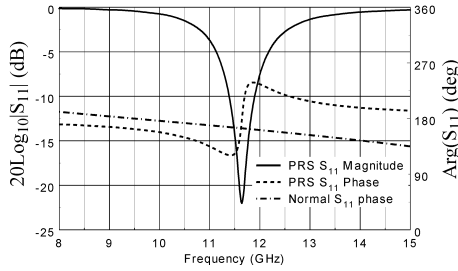


Figure 4. Reflection magnitude and phase of the slot-array PRS.

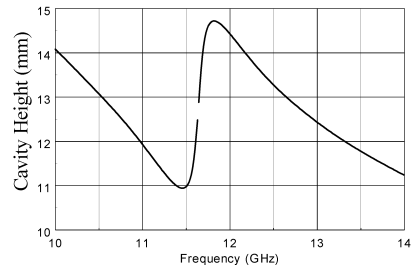


Figure 5. The relationship between the cavity height and cavity resonance frequencies for the slot-array PRS.

to be substituted in Equation (2). For the 10–11.63 GHz frequency range, the calculated cavity height h is only acceptable when $k = 1$. Due to the abrupt phase change at the slot resonance frequency (11.64 GHz), the calculated values of the cavity height by substituting $k = 1$ for $f \geq 11.64$ GHz are not acceptable in practice. However, acceptable cavity height values for $f \geq 11.64$ GHz can be obtained by substituting $k = 2$ in Equation (2). Therefore, the part of the curve for $f < 11.64$ GHz in Fig. 5 is obtained with $k = 1$ and that for $f \geq 11.64$ GHz obtained with $k = 2$.

One should clearly differentiate the *cavity* resonance frequencies from *inclusion* (slots, in this example) or *PRS/FSS* resonance frequencies. The horizontal axis in Fig. 5 represents cavity resonance frequency, which is a variable, because it also depends on cavity height. However, the *inclusion or PRS/FSS resonance frequency* for all these cases is the same, i.e., 11.64 GHz. It is entirely determined by the resonant inclusions in the PRS/FSS.

The most striking feature of Fig. 5 is that, when the cavity height (h) is within the range of 11–14.7 mm, multiple cavity resonance frequency solutions are possible for the same cavity height. That means the same cavity with a fixed height, formed by a *single-band* PRS, can resonate at multiple frequencies, enabling the design of *multi-band* antennas using a single-resonant PRS. The nature of the curve in Fig. 5 suggests that *three* cavity resonance frequencies may be possible for a cavity height in the range of 11–14.7 GHz. However, as explained later, only *two* of these solutions are useful for the operation of an EBG resonator antenna. The solution close to the inclusion resonance frequency is not useful for EBG resonator antenna operation. We will return to this issue later in this section. For the moment, it is sufficient

to say that the resulting EBG resonator antenna is *dual-band*, not tri-band, and one of its operating bands is below the inclusion resonance frequency (i.e., 11.64 GHz in this example) and the other is above the inclusion resonance frequency. By generating curves such as Fig. 5, it is possible to iteratively design PRSs suitable for dual-band antennas that are required to operate in two distinct bands.

Computation of the transmission coefficient $|s_{21}|$ through the equivalent cavity model, shown in Fig. 2(b), reveals useful information on EBG resonator antennas. Obviously the transmission coefficient through the cavity model, i.e., the whole structure shown in Fig. 2(b) (as opposed to just the PRS), is close to 0 dB at frequencies the FSS/PRS (and its image) resonates because all cascaded section in the model has $|s_{21}|$ close to 0 dB at these FSS/PRS resonance frequencies. Nevertheless these frequencies are useless for EBG resonator antenna operation because there is no cavity resonance at these frequencies, and as a result, there is no spreading of the field inside the cavity. (The FSS/PRS actually becomes a non-reflecting surface at its resonance frequency. Without sufficient reflection from the FSS/PRS, the cavity cannot resonate.) The wave simply propagates through the cavity with minimal attenuation. However, the transmission coefficient through the cavity model also peaks and reaches close to 0 dB at other frequencies where the *cavity* resonates, although the $|s_{21}|$ of the PRS is much greater than 0 dB at these frequencies. This high transmission is entirely due to cavity resonance. The cavity efficiently radiates with a narrow beam, forming a high-directivity EBG resonator antenna, at these frequencies.

Let us now analyse the transmission coefficient $|s_{21}|$ through the equivalent cavity model, shown in Fig. 2(b), when the PRS described earlier (and its image) is included in the cavity model. It was computed using CST Microwave Studio, assuming the cavity height (h) is equal to 13.2 mm. These transmission results, plotted in Fig. 6(a), indicate three transmission peaks at frequencies, rf_1 , rf_2 and rf_3 . In Fig. 4, it can be seen that the PRS reflects strongly except at frequency rf_2 . Strong transmission through the cavity is only possible at those frequencies where the cavity resonates. At rf_2 , the PRS is clearly transparent, according to Fig. 4, and hence the transmission through the cavity is strong, though the cavity resonance condition (1) is not satisfied at rf_2 . Hence, the resulting antenna behaves as an EBG resonator antenna around rf_1 and rf_3 but not at rf_2 . This is further verified by the antenna directivity figures presented later. When the field distributions in the cavity were computed at these three frequencies and analyzed, it was found that the field distributions at rf_1 and rf_3 were very similar.

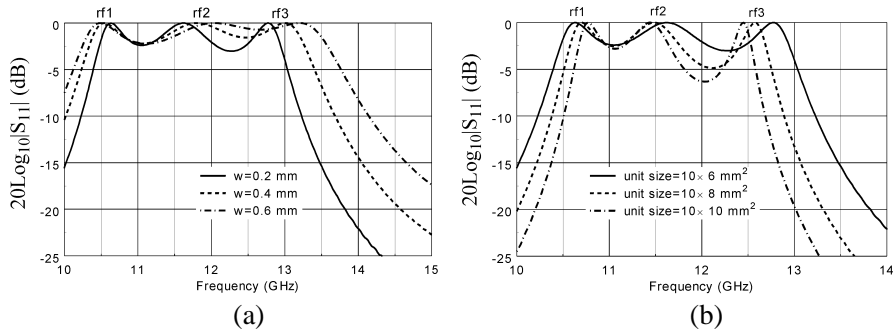


Figure 6. Results of the parametric studies: (a) Effect of the slot width (w) on $|S_{21}|$: unit size = 10×6 mm; (b) Effect of the unit cell width on $|S_{21}|$: $w = 0.2$ mm.

A parametric study of the effects of slot dimensions and the unit cell dimensions on the cavity resonance frequencies has been performed. The effect of the slot width is illustrated in Fig. 6(a). The cavity resonance frequencies rf_1 and rf_3 can be fine-tuned by changing the slot width (w). The smaller the value of slot width, the closer the two frequencies rf_1 and rf_3 . The result of changing the length of the unit cell is indicated in Fig. 6(b). It shows that the positions of rf_1 and rf_3 become closer when the unit cell width is increased.

The design methodology is below:

- The relationship between the slot length and the resonance frequency of the PRS can be approximately estimated by

$$l_r = a \times \frac{c}{2f_r \sqrt{\epsilon_r}} \tag{3}$$

where a , c , l_r , f_r and ϵ_r are a constant, light speed, slot resonant length, PRS resonance frequency and substrate dielectric constant, respectively. The value of the constant a is in the range of 1.1–1.4. It is determined by a lot of factors, such as the thickness of the PRS, the size of the unit cell, the slot width, etc. After the operating bands of the antenna and the material of the PRS are determined, one can first use formula (3) to approximately estimate the slot length, then use CST Microwave Studio to accurately find the length.

- After determining the slot length, the model in Fig. 2(a) and CST Microwave Studio can be applied to determine the transmission and the reflection of the PRS. Using formula (2) to determine the relationship between the cavity height (distance between the PRS

and the ground) and the cavity resonance frequency, as shown in Fig. 5, a dual-band EBG resonant antenna can be obtained. The center frequencies of the two operating bands can be tuned by adjusting the size of the unit and the slot width.

4. DUAL-BAND EBG RESONATOR ANTENNA

A slot-array PRS has been designed following the design method described above. It is placed at a distance of $h = 13.4$ mm from a PEC ground, forming an EBG resonator antenna. The PRS and the ground both have overall dimensions of 110×110 mm² (about $4.5\lambda \times 4.5\lambda$ at 12 GHz). The slot array printed on the bottom surface of the PRS includes 11×11 slots. In this case, the unit cell dimensions are 10×10 mm² and the slot dimensions are 8 mm \times 0.2 mm. The thickness of the PRS dielectric superstrate, made out of FR4/Epoxy, is 0.8 mm. This EBG resonator antenna has been simulated using CST Microwave Studio. For simplicity and numerical efficiency, a horizontal electric dipole (HED) (e.g., an x -polarized HED at the centre of the antenna above the ground) has been included in the simulations, instead of a real feed antenna, to excite the antenna cavity [12]. The antenna directivity and radiation patterns have been computed. Since HED is a broadband excitation, it is possible to obtain results for all the concerned frequencies in a single simulation.

The computed radiation patterns in the E - and H -planes at the cavity resonance frequencies (10.5 GHz and 12.3 GHz) are plotted in Figs. 7 and 8, respectively. As described in the previous section, the positions of rf_1 and rf_3 can be fine-tuned by adjusting the lengths of the slot array and the unit cell. Their positions can also be tuned by varying the cavity height. In this simulation, the antenna achieved the best directivities at rf_1 and rf_3 when the cavity height (h) is 13.4 mm. It can be seen that the level of the side lobe levels in the two planes are below -18 dB at 10.5 GHz and below -20 dB at 12.3 GHz. The predicted directivities at these two frequencies are 18.2 dBi and 20.5 dBi, respectively. The computed directivity within the frequency range of 9.5 GHz–14 GHz is plotted in Fig. 9. Note that the directivity has two maxima at the two cavity resonance frequencies, i.e., $rf_1 = 10.5$ GHz and $rf_3 = 12.3$ GHz. At $rf_2 = 11.4$ GHz, the directivity is low because there is no cavity resonance. The waves pass through the resonating slot array PRS/FSS without much blockage and hence the directivity is close to that of the excitation or the feed antenna. The 3-dB directivity bandwidths of the antenna in the two operating bands are approximately 7.5% and 8.7%, respectively.

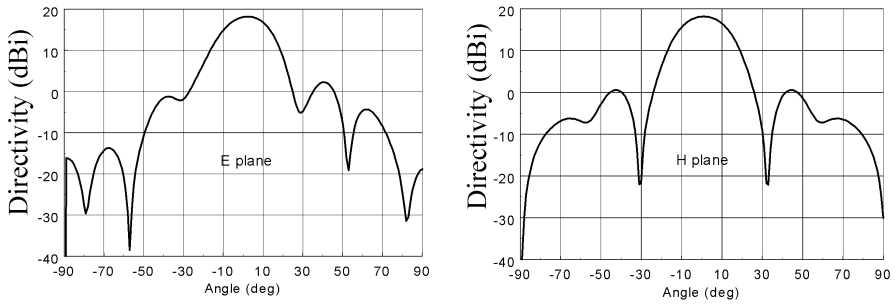


Figure 7. Radiation patterns at 10.5 GHz.

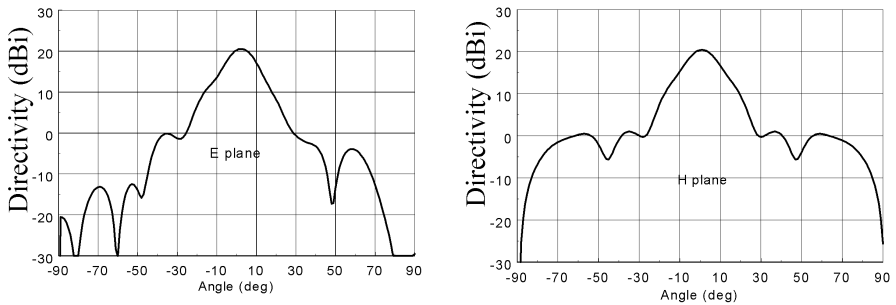


Figure 8. Radiation patterns at 12.3 GHz.

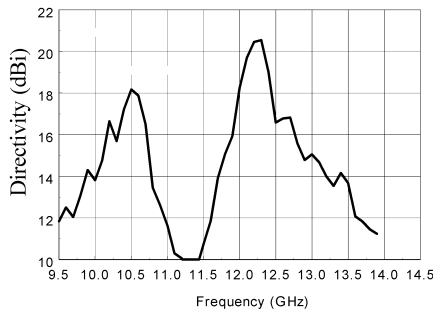


Figure 9. Antenna directivity versus frequency.

5. CONCLUSIONS

The inverted and enhanced gradient of the reflection phase versus frequency curve of partially reflecting surfaces that are made out of resonant inclusions (such as slot arrays) is exploited to develop a new design method for dual-band EBG resonator antennas. Based

on this design method, *dual-band*, high-gain, low-profile, EBG resonator antennas can be designed using *single-layer*, *single-band* partially reflecting surfaces. The key to the design method is the interesting relationship between the cavity height and cavity resonance frequencies. For the same cavity height and PRS, *two* cavity resonance frequencies can be obtained by appropriately designing the PRS/FSS.

Simulations and a design example demonstrate the feasibility of this approach. Simulation results indicate that an EBG resonator antenna, formed by a very simple, single-resonant, single-layer PRS/FSS and a PEC ground, indeed resonates and radiates in two frequency bands. The peak directivities in the two bands are 18.2 dBi and 20.5 dBi, respectively.

ACKNOWLEDGMENT

This research was supported by the Australian Research Council.

REFERENCES

1. Thevenot, M., C. Cheype, A. Reineix, and B. Jecko, "Directive photonic-bandgap antennas," *IEEE Trans. Microwave Techniques and Theory*, Vol. 47, No. 11, 2115–2122, Nov. 1999.
2. Feresidis, A. P. and J. C. Vardaxoglou, "High gain planar antenna using optimized partially reflective surfaces," *IEE Proc. Microwaves Antennas Propagat.*, Vol. 148, No. 6, 345–350, Dec. 2001.
3. Weily, A. R., K. P. Esselle, B. C. Sanders, and T. S. Bird, "High gain 1D EBG resonator antenna," *Microwave and Optical Technology Letters*, Vol. 47, No. 2, 107–114, Oct. 20, 2005.
4. Weily, A. R., L. Horvath, K. P. Esselle, B. C. Sanders, and T. S. Bird, "A planar resonator antenna based on a woodpile EBG material," *IEEE Trans. Antennas Propag.*, Vol. 53, No. 1, 216–223, Jan. 2005.
5. Ge, Y., K. P. Esselle, and Y. Hao, "Design of low-profile high-gain EBG resonator antennas using a genetic algorithm," *IEEE Antennas and Wireless Propagation Letters*, No. 6, 480–483, USA, 2007.
6. Lee, Y., J. Yeo, R. Mittra, and W. Park, "Application of electromagnetic bandgap (EBG) superstrates with controllable defects for a class of patch antennas with spatial angular filters," *IEEE Trans. Antennas Propag.*, Vol. 53, No. 1, 224–235, Jan. 2005.

7. Lee, D. H., Y. J. Lee, J. Yeo, R. Mittra, and W. S. Park, "Design of novel thin frequency selective surface superstrates for dual-band directivity enhancement," *IET Microwaves, Antennas & Propagation*, Vol. 1, No. 1, 248–254, 2007.
8. Rodes, E., M. Diblanc, E. Arnaud, T. Monédière, and B. Jecko, "Dual-band EBG resonator antenna using a single-layer FSS," *IEEE Antennas and Wireless Propagation Letters*, Vol. 6, 368–371, 2007.
9. Pirhadi, A., M. Hakkak, F. Keshmiri, and R. K. Bae, "Design of compact dual band high directive electromagnetic bandgap (EBG) resonator antenna using artificial magnetic conductor," *IEEE Trans. Antennas Propag.*, Vol. 55, No. 6, 1682–1690, Jun. 2007.
10. Hajj, M., R. Chantalat, and B. Jecko, "Design of a dual-band sectional antenna for Hiperlan2 application using double layers of metallic electromagnetic band gap (M-EBG) materials as a superstrate," *International Journal of Antennas and Propagation*, Vol. 2009, 2009.
11. Ge, Y., K P. Esselle, and T. S. Bird, "Designing a partially reflective surface with increasing reflection phase for wideband EBG resonator antennas," *IEEE Antennas and Propagation Society (AP-S) International Symposium*, North Charleston, South Carolina, USA, Jun. 1–5, 2009.
12. Baccarelli, P., P. Burghignoli, F. Frezza, A. Galli, P. Lampariello, G. Lovat, and S. Paulotto, "Effects of leaky-wave propagation in metamaterial grounded slabs excited by a dipole source," *IEEE Trans. Microwave Techniques and Theory*, Vol. 53, No. 1, 32–44, Jan. 2005.